

Applicability of angular orientations of gating designs to quality of sand casting components using two-cavity mould set-up

I. Rajkumar^a, N. Rajini^{b,*}, T. Ram Prabhu^c, Sikiru O. Ismail^d, Suchart Siengchin^e,
Faruq Mohammad^f, Hamad A. Al-Lohedan^f.

^{a, b} *Department of Mechanical Engineering, International Research Centre, Kalasalingam Academy of Research and Education 626126, India.*

^c *Defence Research and Development Organization, Bangalore 560093, India.*

^d *Department of Engineering, Centre for Engineering Research, School of Physics, Engineering and Computer Science, University of Hertfordshire, AL10 9AB, England, UK.*

^e *Department of Materials and Production Engineering, The Sirindhorn International Thai-German Graduate School of Engineering (TGGS), King Mongkut's University of Technology North Bangkok, 1518 Wongsawang Road, Bangsue, Bangkok, 10800, Thailand*

^f *Department of Chemistry, College of Science, King Saud University, Riyadh, 11451, Saudi Arabia.*

*Corresponding author's e-mail: rajiniklu@gmail.com

Abstract

This study aimed to examine integrity of two-cavity sand casting products in relation to angular orientation of gating design. Two angular orientations of 60° and 45° were investigated experimentally and numerically, and compared with the efficiency of a 90° gating system. The FLOW three-dimensional (3D) simulation was conducted to detect smooth filling and describe pattern of molten aluminium LM4 (Al-Si5Cu3) alloy flow. From the results obtained, turbulent flow was observed with vortex, which created larger surface gap to allow air entrapment in molten metal. For both instances, casting discontinuities such as blow holes, pin holes, sponge shrinkage, sand inclusions and dross were observed on the cut 2 mm machined surfaces of the moulded components with various degrees of intensity. Visual analysis, optical microscopy, ultrasonic and X-ray measurements were conducted to check accuracy of the experimental components. All the defect detection methods depicted fewest manufacturing defects with 45° angular orientation, which was attributed to uninterrupted flow of molten metal and low backflow strain. The component with 90° exhibited significant defects, due to turbulent flow, entrapment of air bubbles, lack of mould filling and uneven solidification. These factors consequently caused irregular cracks in the material. Therefore, Practically, 45° angular orientation of gating design with two-cavity mould set-up is hereby recommended for

optimum/best quality sand casting of aluminium LM4 (Al-Si5Cu3) alloy components, as required in many manufacturing companies.

Keywords: Sand casting, Gating system, Numerical simulation, Manufacturing.

1. Introduction

The development of technologies in the field of small-scale casting industries is necessary to produce high quality products at low costs. Majority of small businesses depend on traditional methods with challenges of achieving high efficiency. Therefore, manufacturing capabilities of achieving complex shapes utilise tailored method parameters, because traditional casting process cannot be shut down [6]. Normally, in sand casting, movement of molten metal filled into a mould cavity through gravitational force via the gating and runner mechanisms is a vital process to determine solidification process. Non-uniform metal flow may result in defects, due to irregular solidifications and mould filling [7]. Furthermore, feeding system in sand casting process is one of the most important variables in determining product consistency by monitoring casting shrinkage faults, surface sink and internal cracks [9-11]. Also, feeding system for a casting part with an experimental set-up contains a runner, liquid basin, sprue, well runners, gates and slag traps.

To stop shrinkage, factors such as the shape and size of the feeder and feeder neck, the position of the feeder, insulating sleeves and covers, fins and chills have been included in the nature of the feeder device [13-15]. Hence, a perfect gating device may guarantee smooth, full and uniform filling in less time, allowing for identification and removal of several defects. It played an important role in the manufacture of casting parts [16]. The traditional gating resulted in higher air entrainment and irregular flow. Some previous studies used a modified design in terms of geometric criteria with three separate layouts. As a result, modifications such as runner measurements, runner curvature, down sprue point of link runner, cross-section of down sprue dimensions and in-gate as well as place dimensions have been studied. Feeding layouts were observed to increase consistency. Finally, optimal streamlined feeding mechanism based on simulation results was observed. Also, the results showed decrease in air entrainment and turbulence movement with limited content consumption, allowing for an increase in casting yield from 73 to 77% [17]. To obtain the best feeder configuration, the process parameters must be changed throughout the design phase. Accordingly, many software tools are exclusively designed for the casting industries to address many issues by governing the real time process

effectively. However, various casting simulation tools act differently, depending on the built-in availability of resources when it comes to achieving the desired goal.

Moving forward, applicability of modelling techniques in small-scale manufacturing, as a cost-effective method is still being embraced today. Consequently, industries are trying to achieve 'right the first time' approach to minimise the time consumptions via direct selection of best combination of parameters. This method, however, is difficult to accomplish in the real-time sand casting process. Therefore, many trial-and-error processes are also used by small-scale enterprises. On the other hand, large-scale companies have started adopting modelling methods that have demonstrated less time intensive in selecting the optimum parameters for suitable conditions. Various gating device designs were analysed along with experimental and simulation performances on the quality performances of casting products [12]. The simulation was performed primarily to find the optimal gating configuration, which outlined the findings to obtain smooth surface and good internal consistency [8].

Furthermore, computational modelling was used to provide valuable insights into molten metal flow, heat transfer, solidification and mould filling in this current investigation, similar to previous studies [1,2]. Also, the simulation process aimed to mitigate the casting design phase by refining the casting conditions, minimising material waste and human resources. To produce casting efficiency, the solidification character of automobile parts and filling were used to create a simulation method [3-5]. Our research group has conducted studies on different feeding designs for various casting product applications. However, direction of the gating normal to the main runner was considered in those works. The results depicted backflow of molten metal in both experimental and numerical simulation approaches, which created formation of discontinuities in the casting products [18-20].

To the best of our understanding, the consequence of varying direction of gating configuration with respect to the main runner has not yet been investigated, especially for various two-cavity structures. Based on this research gap, this current work was focused on effects of various gating angular orientations on quality of casting products, using two-cavity moulds with respect to the main runner. FLOW three-dimensional (3D) simulation software was employed to understand the flow of a molten metal in relations to mould filling and temperature distribution. The casting products were produced experimentally, considering sand casting method and various gating orientations based on the simulation parameters. Furthermore, manufacturing defects or flaws in the fabricated casting products were examined using a number of non-destructive examination techniques, which included microscopy analysis, visual and X-ray inspections.

2. Material and methods

2.1. Material used

A typical aluminium LM4 (Al – Si5Cu3) alloy was used to explain the movement of molten metal in sand casting phase at various angular orientations of the gating design or system (Fig. 1). Table 1 presents the chemical composition of the LM4 (Al – Si5Cu3) casting material. This aluminium alloy is widely available and largely used materials in various applications, such as spacecraft, aircraft, ship components, especially those that fill the hull with cargo, trains and personal vehicles.

2.2. Modelling details of mould pattern

For two-cavity moulding configuration, geometric structure of the whole mould pattern was modelled using CREO 3.0 software package. Measurements of various sections of the moulding systems, such as the sprue frame, sprue of minimum diameter of 12 mm, maximum diameter of 22 mm, key runner of 15 x 15mm, gate of 18 x 9 mm and component of 50 x 50 mm were used to build the two-cavity moulding set-up. The modelling data were then translated into stereolithography (STL) files. It was used as an input for the simulation run by the FLOW 3D programme. The angular orientation of the gating mechanism was supposed to play an important role in flow simulation and to have an impact on casting consistency. Additionally, the flow behaviour between components, such as sprue base to runner and main runner to gating as well as the flow of molten metal after the backflow pressure can be observed. Fig. 2 depicts both top (plan) and isometric views of the mould designs. The top views of Figs 2(a)-(c) show the symmetrical angular orientations of the gating designs at different angles of 90°, 60° and 45°.

2.3. Numerical simulation

STL file of the 3D model was directly imported to FLOW 3D simulation software. Model was meshed using suitable node size, and simulation was performed with the FLOW 3D software to simulate temperature and velocity. Some important flow input parameters used are

presented in Table 1. Molten metal was poured into each mould set-up in z-position on sprue top to analyse the temperature distribution and mould filling in the two-cavity system.

2.4. Fabrication of two-cavity mould using sand casting process

Casting pattern was fabricated by using wooden material according to the geometric design of two-cavity component, as previously shown in Fig. 1. It was made up of a pouring basin, a tapered sprue with a circular cross-section, a runner with a constant square cross-section and two gates with same square cross-section portion. The experimental arrangement has a gating ratio of 1.0: 2.0: 5.6. One end of the main runner was mounted in the sprue and two components were arranged in opposite directions at 90° to the centre line of runner axis for the first series of experiments. The centre line of the gate at both side was attached to the runner at an angle of 60° in the second series of experiments. The centre line of the gate at both sides was attached to the runner at an angle of 45° in the third series of experiments. The silica sand was used to prepare three different mould set-ups. Aluminium alloy (LM4/A319) was melted at the furnace temperature of 800 °C before pouring into the mould. Then, the molten metal was poured into the mould at pouring temperature of 720 °C and atmospheric pressure of pre-heating of 140 °C of the mould cavity to avoid the sudden cooling when entering into the mould cavity. This experiment was repeated three times for each angular gating design. Finally, it produced 6 components per case and total components of 18 to ensure that effects of gating angles on the quality of the products were analysed.

3. Result and discussion

3.1. Theoretical flow analysis in the feeder components

To explore the flow parameters in various sections of the feeder, the following assumptions were considered with suitable scientific justifications:

1. Aluminium molten metal was considered as incompressible fluid.
2. Dynamic viscosity of the molten metal was neglected.
3. Back pressure was not considered.

3.1.1. Vertical section

The entire sprue part, including both sprue basin and rod, was considered according to the geometry used in the experimental study to determine the flow parameters (Fig. 3).

Accordingly, the volume of sprue basin was calculated, using Eq. (1)

$$V = l \times b \times h \quad (1)$$

Where l , b and h represent length, breadth and height of the sprue basin.

The time taken by the fluid top surface to reach section 1 was calculated under the uniform acceleration condition, using the following equations. The initial velocity of the fluid surface was considered as zero.

$$h = u_t + \frac{1}{2}gt^2 \quad (2)$$

$$\text{Discharge, } Q = \frac{V}{t} \text{ (m}^3\text{/s)} \quad (3)$$

$$\text{Mass flow rate, } \dot{m} = \rho Q \text{ (kg/sec)} \quad (4)$$

The velocities at sections 1 and 2 were calculated, using the constant volume of flow rates; Eqs 5 and 6, respectively:

$$Q_1 = A_1V_1 \quad (5)$$

$$Q_2 = A_2V_2 \quad (6)$$

The pressure of the molten metal acting in the section 1 was calculated by using Eq. (7);

$$P_1 = \rho gh \quad (7)$$

The force equilibrium Eq. (8) was applied by considering the forces acting along the vertical axis,

$$\dot{m}(v_1 - v_2) = P_2A_2 - P_1A_1 - W_m \quad (8)$$

Where,

P_1 and P_2 represent molten metal pressures at sections 1 and 2, respectively.

A_2 and A_1 denote the area cross-sections at sections 1 and 2, respectively.

W_m stands for weight of the liquid/molten metal,

Therefore,

$$W_m = \rho g V_m = \rho g \frac{\pi}{12} (D_1^2 + D_2^2 + D_1D_2)h \quad (9)$$

Where,

ρ = liquid density of the aluminium,

g = acceleration due to gravity,

D_1 and D_2 = diameters at sections 1 and 2, respectively.

Additionally, it was a convergence sprue, therefore increased velocity and decreased vacuum pressure (below atmospheric pressure) were determined as expected. This vacuum pressure was acted as driving force to push the molten metal in the runner. It was designed to have a moderate length to decrease the turbulence and splashing of molten metal. Furthermore, an optimum runner length was chosen to increase the yield of the casting.

3.1.2. Horizontal section

Based on geometry of the gating systems used in this work, force analysis was performed assuming the principle of super-position to find out the mass flow rate in each branch of the gating system, as shown in Fig. 4. Normally, this principle was applied to the single plan system and therefore the branches of the gating system were lying on the same plan in the feeder design. Accordingly, angular orientation of gating system was assumed as a bend pipe during force analysis to determine the net force acting along x- and y-directions, as in cases 1 and 2 respectively and discussed subsequently.

Case 1:

Equilibrium of force along x-direction in the bend pipe of 60° inclination to the horizontal,

$$P_1A_1 - P_2A_2 \cos 60 - F_x = \dot{m} (V_2 \cos 60 - V_1) \quad (10)$$

$$F_x = 0.466 - 0.00081P_2 \quad (11)$$

Equilibrium of force along y-direction in the bend pipe at 60° inclination to the vertical is shown in Eqs (12) and (13):

$$-P_2A_2 \cos 60 - F_y = \dot{m} V_2 \sin 60 \quad (12)$$

$$F_y = 0.00914P_2 - 0.0935 \quad (13)$$

Case 2:

Equilibrium of force along y-direction in the bend pipe at 45° inclination to the horizontal is similarly shown in Eqs (14) and (15):

$$P_1A_1 - P_2A_2 \cos 45 - F_x = \dot{m} (V_2 \cos 45 - V_1) \quad (14)$$

$$F_x = 0.52 + 0.001145P_2 \quad (15)$$

Also, equilibrium of force along y-direction in the bend pipe at 45° inclination to the vertical is shown in Eqs (16) and (17):

$$-P_2 A_2 \cos 60 - F_y = \dot{m} V_2 \sin 45 \quad (16)$$

$$F_y = 0.444 - 0.000809P_2 \quad (17)$$

Horizontal force acting in the horizontal section of the runner is given as Eq. (18):

$$P_1 A_1 - F_x = \dot{m} (V_1) \quad (18)$$

The amount of flow rate at the branches can be calculated from the total amount of flow rates in the inlet pipe, as shown in Fig. 5 and Eq. (19):

$$Q_T = Q_1 + Q_2 + Q_3 \quad (19)$$

Due to the symmetry of the geometry of the branch, $Q_1 = Q_3$, hence,

$$Q_T = 2Q_1 + Q_2 \quad (20)$$

$$Q_1 = A_1 V_1 = A_1 V_2 \cos 45 \quad (21)$$

$$Q_2 = A_2 V_2 \quad (22)$$

$$V_1 = V_2 \cos 45 \quad (23)$$

The filling time in the casting can be calculated, using Eq. (24),

$$\text{Pouring time} = \frac{\text{Volume of casting}}{\text{Area of cross section at the gate} \times \text{velocity at the gate}} \quad (24)$$

Eqs (19) – (24) were used to generate process parameters/data obtained and presented in Table 2.

According to the theoretical study, the difference in fluid discharge was observed in the inclined branch of channels during the first molten metal flow in the runner direction. The velocity obtained at the choke point was used as the inlet velocity in the runner's horizontal portion. Furthermore, the design also experienced an expansion of the runner to reduce the momentum of the metal and, as a result, the intensity of the turbulence. The molten metal flowed into three distinct sections: two inclined branches of passage with varying angles of inclination with the horizontal, and one straight channel of the same area of cross-section as the inlet passage (Fig. 5). Together with the straight outlet tubing, two inclined passages of 60° and 45° were branched. The study results showed that no fluid was observed to enter the 90°

branch pipe, since it was suddenly deviated from the flow of molten metal bath. However, in reality, a very small volume of discharge could have reached. In the case of inclined channels, partial fluid with significant volumes of discharges of 25 and 20% entered into the in-gate, as observed. Since the geometry of 45° inclined pipes fell in the path of the molten metal, a greater volume of fluid entered than the 60° inclined pipes. On the other hand, larger amount of first liquid metal was hitting at the end of the horizontal runner, returning back with the back pressure and colliding with the front flood of metal. The turbulent flow was supposed to occur at the stage of fluid collision. The volume of fluid that returned after reaching the end of the horizontal runner determined the speed of the turbulence. As a result, in case of 90° and 60° inclined tubing, a considerable volume of return fluid occurred. There was just a small amount of fluid entering the inclined channels during the first metal flow. Furthermore, if there is more back streaming, the relative velocity of the molten metal was supposed to increase. Consequently, the influence of turbulence might be greater in the case of the 90° branch of channels, accompanied by the 60 and 45° designs.

3.2. Numerical simulation

FLOW 3D modelling programme was used to carry out the computational simulation in all the three cases. Table 3 shows details of the boundary conditions, material selection and their molten metal properties, preheat temperature and mesh used. The temperature and velocity simulation performances of all the three types of gating designs are shown in the first and second columns of Fig. 6. The changing colour legends reflected the magnitudes of the related variables at various locations during flow analysis. As a result, in the profiles displayed in Fig. 6, the red colour represents the greatest temperature and velocity disparity, whereas the blue colour represents the smallest. The temperature and velocity flow variances for all the three situations were measured at the same period of 2.55 seconds to equate flow efficiency to gating orientations.

In addition, the first feed of metal from the sprue choked and broke into two sides of the runner in the first case of 90°. The first metal travelled in the left extension section solidified with the slags. Impurities were found in the original metal, reducing the likelihood of casting defects. Furthermore, the flow on the right side of the runner lost kinetic energy when it travelled through three parallel paths, two of which were normal to the flow direction. As observed in Fig. 6(a), the volume of fluid entering the casting took a long time at 90°, and the solidification within the casting also took a long time. Because of this delay, solidification

might have started or occurred in the runner, obstructing the flow of molten metal in the casting. A slight volume of molten metal entered the casting at a set point in the case of 60° castings (Fig. 6b), and a further rise in mould filling was observed in 45° castings (Fig. 6c). Because of the non-uniform flow of metal within the casting, dendrites might have developed in the solidification front, causing a discontinuity between the hot spot of the metal and neighbouring solidification regions. Inadequate feeding was observed within the casting at 90° gating system, which could result to macro/micro porosity and surface shrinkage, among other casting defects. Because of the mass feeding of metal, standardised solidification occurred at about 53 °C at the bottom of the casting in the case of a 45° gating branch. Because of the benefit of gating orientation, both temperature and gradients were observed to be elevated in this situation.

Besides, the velocity profile showed a rise in velocity at the outlet of the sprue choke region in both cases, and the final velocity was obtained to be negligible at the end of the horizontal runner. The collision between the back flow of liquid and the front feed of metal, on the other hand, would have triggered a rise in relative velocity at a point or junction. In the case of a 90° branched channel, the development of turbulence can often be observed with the greater surface region. The greater surface region of the turbulence was observed both at the runner and at the gating exit. This would have resulted to formation of oxide layers as well as possibility of air entrapment in the molten metal, which solidified as air bubbles within the product.

Moving forward, from 60° gating configuration, the surface region of the turbulence was found to be reduced within the area of the main runner and almost nullified at the gate exit. This was possible, because backflow reduced the amplitude of relative velocity, which in turn reduced the influence of turbulence. The inclined channel experienced a transformation from chaotic to laminar flow, which can be attributed to smooth mixing of front and reverse flows. In addition, a faster casting filling was observed in this case when compared with 90° branched channels. Similarly, the inclined channel at 45° angle exhibited less turbulence, owing to a greater degree of flow entry during the initial flow of metal. In reality, no turbulence impact was observed in the feeder design environment, implying a smooth flow of metal accumulation. Also, simple casting filling occurred with standardised solidification and low number of casting defects. The maximum amount of filling within the casting for a given period was determined for 45, 60 and 90° gating orientations.

The same geometrical parameters used in the simulation process were used in the experimental work for all forms of gating architectures. The volumetric sum of mould filling was measured and compared with the numerical results obtained. Initially, 70% of the weight of the melting mould casting part was poured into the system to estimate the amount of molten

metal flow in the casting. Only a portion of the liquid was used to accomplish incomplete filling of the component, therefore flow rate in the casting may be determined for all the situations. According to the experimental results obtained, 45° gating channel recorded the greatest volume of movement, accounting for 79% of the total casting volume. Similarly, the amount of flow estimated from 60° and 90° gating designs were 74 and 69%, respectively. The same measurement was taken from the simulation data, which indicated a significantly improved amount of metal relative to the experimental results, but the maximum volume of 90% was achieved only with 45° gating channel. The obstruct obtained in real-time practice when accounting for noise variables cannot be considered in the simulation phase. The sequence of the outcomes obtained from both instances, however ensured the actual flow phase of different authentications.

3.3. Macroscopic failure analysis

To predict the internal failure of the casting materials, macroscopic images were taken using different techniques at their machined top surfaces, cut-sections and bulk materials. The experiments were repeated in three times for all the three types of gating designs and a sum of 18 components were considered for the defect verification. All the samples were machined 2 mm at each side before examination. Fig. 7 depicts optical views of the casting elements taken at the machined top surfaces of all the three gating designs. The surface of 90° gating design showed a lot of macro porosities and sand inclusion. Both of these flaws occurred at the casting edge, which can be attributed to the splashing of a small amount of liquid at side wall of the casting. In case of 60° gating style, Fig. 7(b) explicitly shows a small number of arbitrarily directed pin holes and air bubbles. There was a lot of turbulence at the runner area, which might be a path for air to enter and create oxide layers on the casting outer surface. Conversely, gating design of 45° produced a clean and smooth surface with no significant flaws, as depicted in Fig. 7(c). This can be traced to the diminishing velocity at the point of collision, hence laminar form of metal flow occurred.

Both 90° and 60° gating designs indicated each 4/6 (nearly 67%) defected components after microscopic examination of 6 components in each event. Angular gating system of 45° recorded only 2/6 (approximately 33%) defected components, and its defect occurred in an appropriate area.

3.4. Optical inspection

Every part was split into two halves and the casting defects were analysed to determine the failure of the components at their mid-sections. The morphology of the cut segment was captured on both sides using a Motic optical microscope, digitally operated by Plus 2.0 mL image processing software package. According to Fig. 8, 90° gate orientation mould set-up created an irregular structure on cut-section of the casting, due to inconsistent metal filling, significant scale shrinkage defects and irregular hard spots. Furthermore, a spherical and elongated cavity defect was observed in both sides of the cut-segment of the 60° gate orientation mould configuration, as shown in Fig. 8. This defect might have been induced by the influence of turbulence and discontinuous movement of molten metal when entering into the cavity, leading to an insufficient solidification. However, 45° gate orientation mould set-up demonstrated minimal defects on both outer and inner surfaces (Fig. 8).

The defect-free surfaces of the component of intermediate section of 45° gating design implied that the flow of molten metal in the cavity was uniform. Also, the change to laminar flow occurred after the depletion of kinetic energy with less fluid effect at the juncture.

3.5. X-ray examination

Radiography test was conducted in Coimbatore with a Carestream system radiography (CR) unit at 160 peak kilovolts, wielded by discovery and prudence of 25 secs and current of 5mA. The aim of the test was to investigate into the internal flaws in the bulk components of all the three types of gating systems. Pin and blow holes were observed from the X-ray images obtained from the castings of both 90° and 60° gating designs, as shown in Figs 9(a) and (b). This manufacturing defects can be attributed to condensed gas or air trapped by the metal. Many of these discontinuities were discovered to be smooth-walled, rounded cavities with spherical, elongated and/or flattened shapes. It could have happened due to lack of permeability in the mould sand, inadequate venting and an incorrect gating configuration. Furthermore, closed shrinkage, a form of discontinuity, was observed in all the three cases as dark spots in the radiographic photographs (Fig. 9). In general, shrinkage defects in different shapes, although in all cases, occurred because molten metal shrank after it solidified in all areas of the final casting. The X-ray examination depicted four forms of shrinkage defects: (1) cavity, (2) dendritic, (3) filamentary and (4) sponge. Consequently, at least two of these kinds of flaws could be observed from the castings produced by 90° and 60° gating designs in the shape of very fine lines or narrow elongated cavities. At certain locations, a continuous system of linked lines or branches of varying duration, distance and intensity, or as a network, was often present. The areas of lacy texture with diffused outlines and dendritic were observed, due to the

volumetric contraction of molten metal and existence of unfavourable temperature gradient, which depended on absence of directional solidification. Besides, with these two cases of 90° and 60° gating designs, lack of fluidity might have contributed to the intermediate solidification of metal in the runner and gating. The restriction in the path of flow of molten metal could have created lack of metal filling in the cavity. Case of 45° gating design was characterised with a small amount of dark region, as observed and shown in Fig. 9. It indicated absence of dendrites and other defects. The smooth flow of molten metal and less intensity of turbulence can facilitate the uniform solidification process, which was associated with optimum 45° gating design and its best quality component or product.

4. Conclusion

The impact of angular orientation of gating design on casting efficiency of a two-cavity sand casting method has been investigated. The direction of gating was observed to monitor the strength of turbulence caused by metal reverse flow. The sudden lateral shift of gating, perpendicular (at 90°) to the flow direction, caused irregular mould filling and significant instability at the runner region's centre section and entry of the gating. The turbulence impact was reduced when the angles of inclination were reduced to 60° and 45° with respect to the horizontal axis. Significant gaseous defects, including blow and pin holes, characterised by closed shrinkage cavities were evidently visible at the cut and top portion of 90° and 60° gating designs, under different pressure.

Owing to the lack of lateral solidification, the dark regions observed from X-ray inspection depicted dendrite, filament and sponge produced shrinkage castings. Gating system of 45° recorded 6.45 and 17.80% greater amount of flow than 65° and 90° gating designs, respectively. Summarily, 33% of the cast parts was defective with 90° and 60° gating designs. While, 80% of the cast components was defect-free or flawless with 45° gating design. Significantly, it was evident that 45° angular gating orientation performed best, hence it is recommended for optimum quality two-cavity sand casting process in manufacturing industries to maximise both productivity and profitability.

References

- [1] Ling Y, Zhou J, Nan H, Yin Y, Shen X (2017) A shrinkage cavity prediction model for gravity castings based on pressure distribution: A casting steel case. *J Manuf Proc* 26:433-445.
- [2] Fu Y, Wang H, Zhang C, Hao H (2018) Numerical simulation and experimental investigation of a thin-wall magnesium alloy casting based on a rapid prototyping core making method. *Int J Cast Metals Res* 31(1):37-46.
- [3] Chen LQ, Liu LJ, Jia ZX, Li JQ, Wang YQ, Hu NB (2013) Method for improvement of die-casting die: combination use of CAE and biomimetic laser process. *Int J Adv Manuf Technol* 68(9-12):2841-2848.
- [4] Zhang S, Li J, Kou H, Yang J, Yang G, Wang J (2016) Numerical modelling and experiment of counter-gravity casting for titanium alloys. *Int J Adv Manuf Technol* 85(5-8):1877-1885.
- [5] Chen JH, Hwang WS, Wu CH, Lu SS (2011) Design of die casting process of top cover of automobile generator through numerical simulations and its experimental validation. *Int J Cast Metals Res* 24(3-4):163-169.
- [6] Fu PX, Kang XH, Ma YC, Liu K, Li DZ, Li YY (2008) Centrifugal casting of TiAl exhaust valves. *Intermetallics* 16(2):130-138.
- [7] Hong CP (2004) Computer modelling of heat and fluid flow in materials processing. CRC Press.
- [8] Wenming J, Zitian F (2014) Gating system optimization of low pressure casting A356 aluminum alloy intake manifold based on numerical simulation. *China Found* 1(2):119-124.
- [9] Mohiuddin MV, Krishnaiah A, Hussainy SF, Laxminarayana P (2016) Influence of process parameters on quality of Al7SiMg alloy casting using statistical techniques. *Materials Today Proceed* 3(10):3726-3733.
- [10] Rajkolhe R, Khan JG (2014) Defects, causes and their remedies in casting process: A review. *Int J Research Advent Technol* 2(3):375-383.
- [11] Chen JC, Buddaram Brahma AR (2014) Taguchi-based six sigma defect reduction of green sand casting process: An industrial case study. *J Enterprise Transform* 4(2):172-188.
- [12] Sikorski S, Dieckhues GW, Sturm JC (2012) Systematic optimization of aluminum sand casting gating systems. *American Foundry Soc* 120:13-21.

- [13] Renukananda KH, Ravi B (2016) Multi-gate systems in casting process: comparative study of liquid metal and water flow. *Mater Manuf Proc* 31(8);1091-1101.
- [14] Reis A, Houbaert Y, Xu Z, Van Tol R, Santos AD, Duarte JF, Magalhaes AB (2008) Modelling of shrinkage defects during solidification of long and short freezing materials. *J Mater Proc Technol* 202(1-3):428-434.
- [15] Reis A, Xu Z, Tol RV, Neto R (2012) Modelling feeding flow related shrinkage defects in aluminum castings. *J Manuf Proc* 14(1):1-7.
- [16] Modaresi A, Safikhani A, Noohi AMS, Hamidnezhad N, Maki SM (2017) Gating system design and simulation of gray iron casting to eliminate oxide layers caused by turbulence. *Int J Metal Casting* 11(2):328-339.
- [17] Hahn I, Jorg CS (2010) Autonomous optimization of casting processes and designs. Proceedings of the 69th World Foundry Congress, Hangzhou, China, Oct. 16-20.
- [18] Rajkumar I, Rajini N, Alavudeen A, Prabhu TR, Ismail SO, Mohammad F, Al-Lohedan A (2021) Experimental and simulation analysis on multi-gate variants in sand casting process. *J Manuf Proc* 62:119-131.
- [19] Rajkumar I, Rajini N (2021) Influence of parameters on the smart productivity of modern metal casting process: An overview. *Mater Today Proc* <https://doi.org/10.1016/j.matpr.2021.03.003>
- [20] Rajkumar I, Rajini N (2021) Metal casting modelling software for small enterprises to improve efficacy and accuracy. *Mater Today Proc* <https://doi.org/10.1016/j.matpr.2021.02.542>

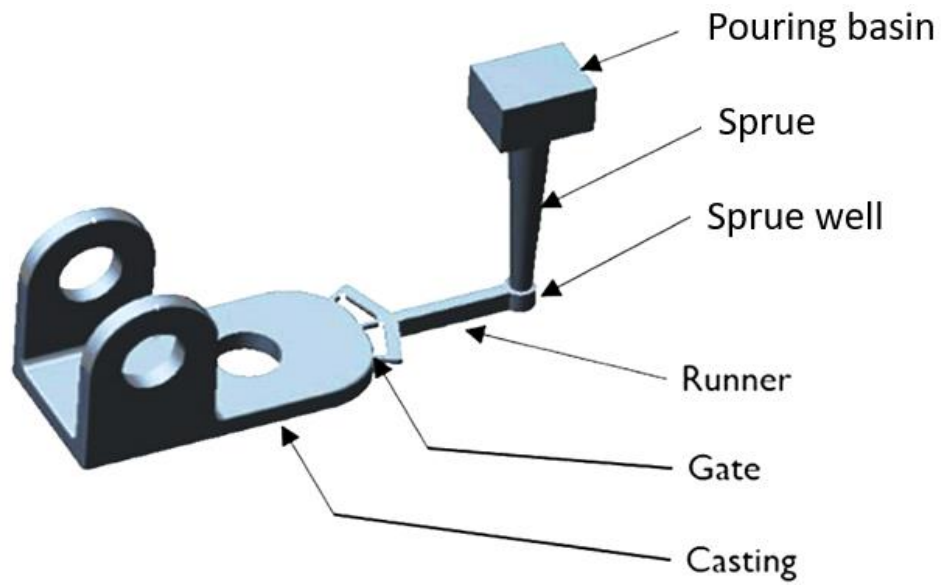


Fig. 1. Components in a typical gating system.

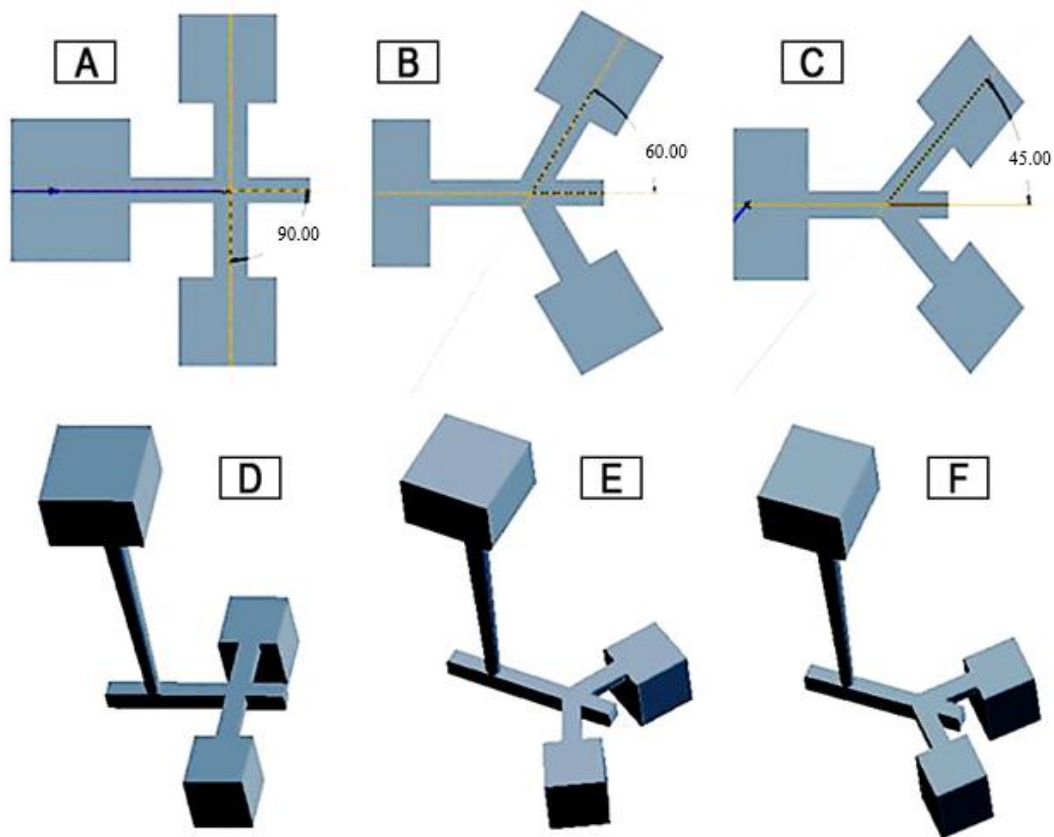


Fig. 2. Two-cavity component in three different gating orientations and their isometric views of (a) and (d) 90°, (b) and (e) 60° as well as (c) and (f) 45°, respectively.

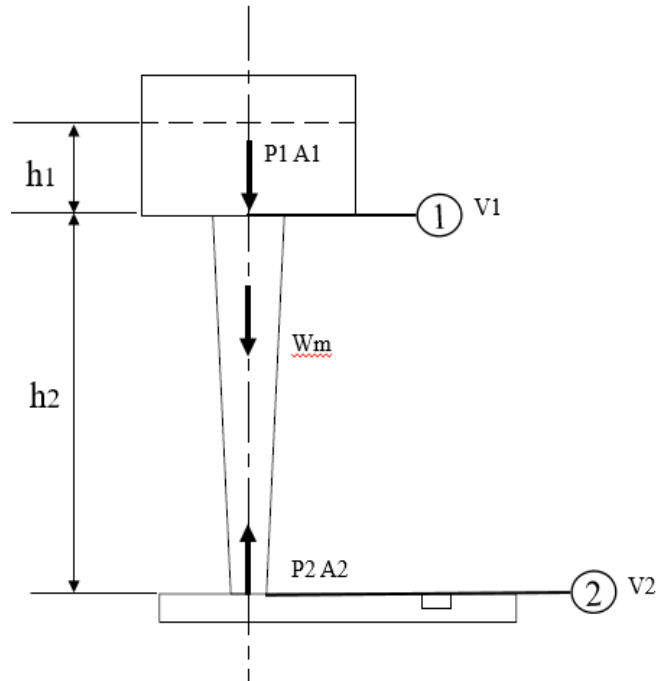


Fig. 3. Schematic representation of vertical geometry of the sprue basin and rod.

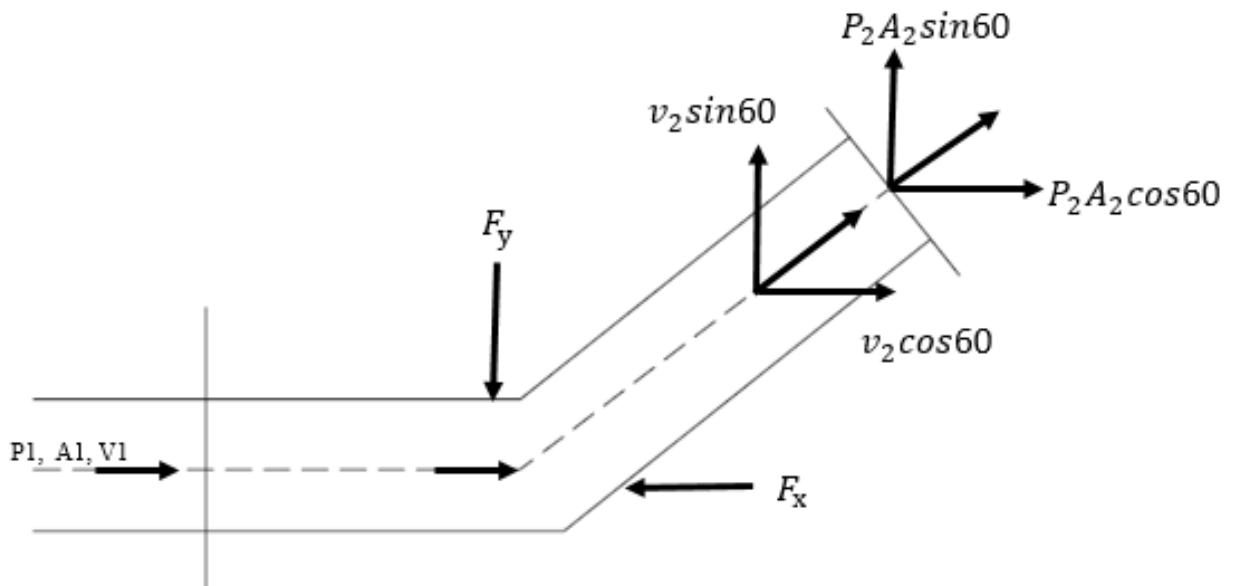


Fig. 4. Force analysis of the angular orientation of gating system assumed as bent pipe.

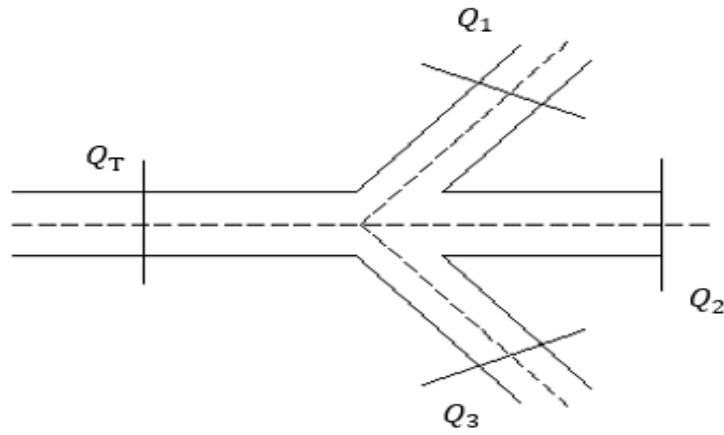


Fig. 5. Illustration of total amount of flow rate at the branches in the inlet pipe.

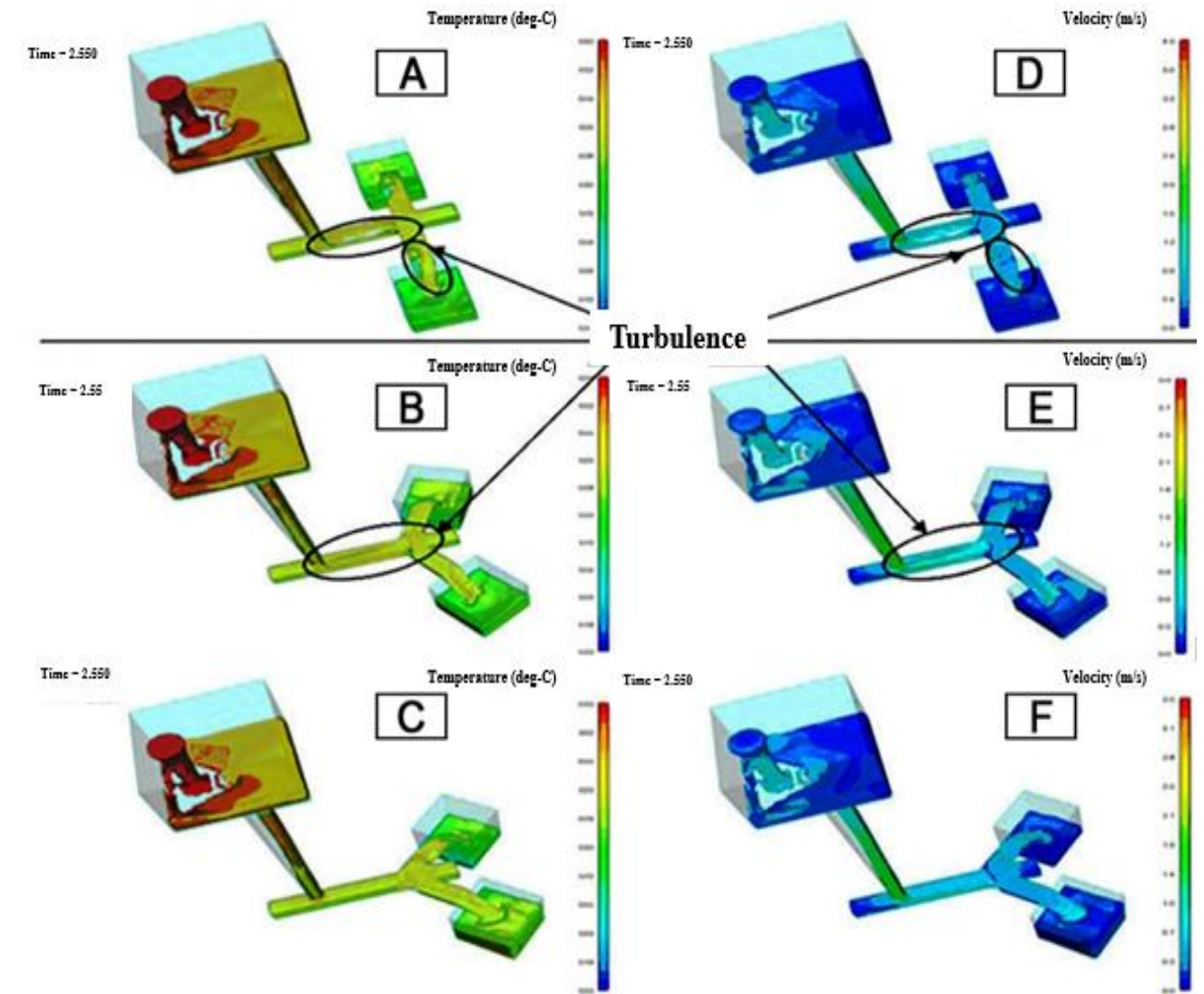


Fig. 6. Flow simulation behaviours of two-cavity angle gating systems with temperature and velocity distributions of (a) and (d) 90°, (b) and (e) 60 ° as well as (c) and (f) 45°, respectively.

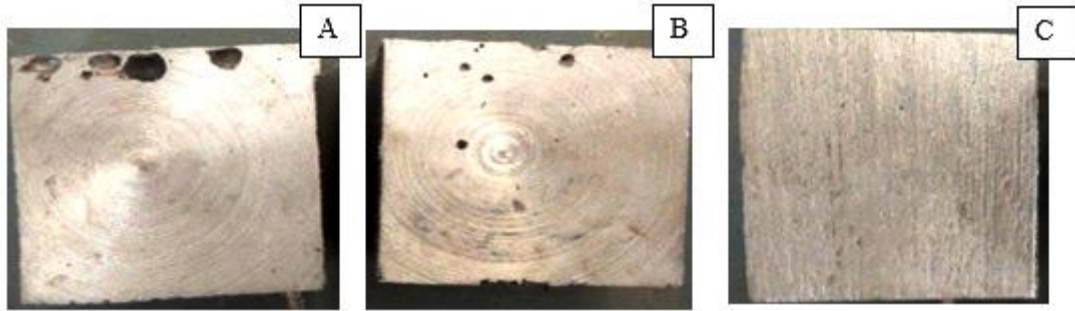


Fig. 7. Visual defect examination of 2 mm machined component surfaces of (a) 90°, (b) 60° and (c) 45° gating systems or designs.

Mould set-up/ angle of orientation	High resolution photographic images		Optical microscopic images	
	Component 1	Component 2	Component 1	Component 2
90°				
60°				
45°				

Fig. 8. Component cut-sections of 90°, 60° and 45° gating systems, showing their photographic images (left) and their optical microscopic images (right).

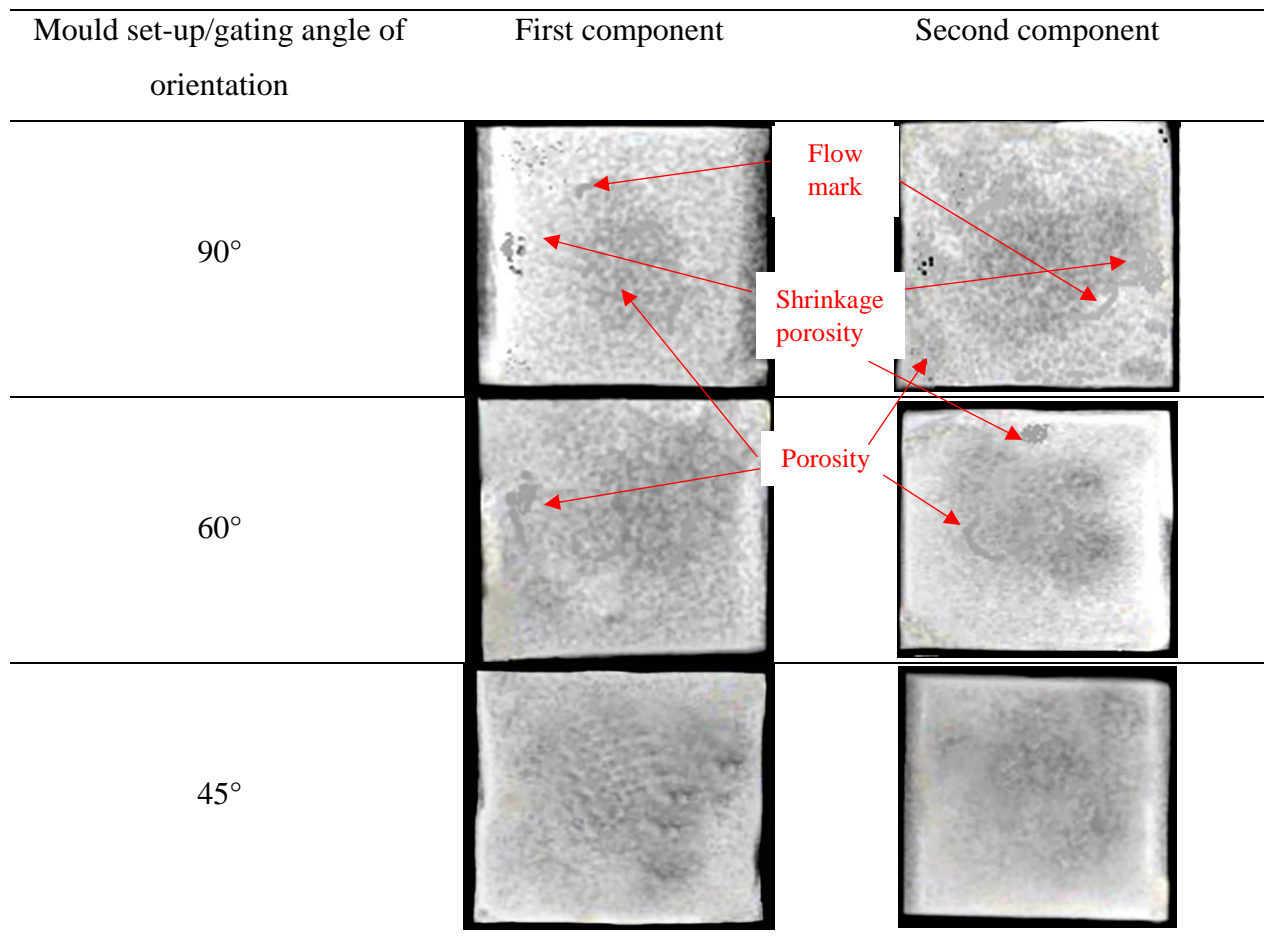


Fig. 9. X-ray micrographs of mould set-ups/gating angles of 90°, 60° and 45° orientations.

Table 1

Chemical composition of LM4 (Al – Si5Cu3) material.

Elements	Cu	Mg	Si	Fe	Zn	Mn	Ti	Pb	Ni	Sn	Al
Percentage (%)	4.00	0.15	6.00	0.80	0.50	0.60	0.20	0.10	0.30	0.10	87.20

Table 2

Process parameters/data obtained.

S/No	Velocity, v (m^3/s)		Discharge, Q (m^3/s)		Mass flow rate, \dot{m} (kg/s)		Percentage (%)
1.	Nil		Q_T	4.57×10^{-4}	\dot{m}_T	1.08	100
Vertical section							
2.	v_{v1}	1.3200	Q_{v1}	4.57×10^{-4}	\dot{m}_T	1.08	100
3.	v_{v2}	4.0400	Q_{v2}	4.57×10^{-4}	\dot{m}_T	1.08	100
Horizontal section and angle orientations							
	v_{h1}^{45}	0.0710	Q_{h1}	1.15×10^{-4}	\dot{m}_1	0.273	25.27
45°	v_{h2}^{45}	0.1000	Q_{h2}	2.25×10^{-4}	\dot{m}_2	0.534	49.44
	v_{h3}^{45}	0.0710	Q_{h3}	1.15×10^{-4}	\dot{m}_3	0.273	25.27
	v_{h1}^{60}	0.0059	Q_{h1}	9.55×10^{-4}	\dot{m}_1	0.220	20.03
60°	v_{h2}^{60}	0.1180	Q_{h2}	2.95×10^{-4}	\dot{m}_2	0.700	64.81
	v_{h3}^{60}	0.0059	Q_{h3}	9.55×10^{-4}	\dot{m}_3	0.220	20.03

Table 3

Input flow parameters.

S/No	Parameter	Units	Aluminium alloy (LM4)
1.	Velocity	m/s	2.69
2.	Pouring temperature	°C	720
3.	Density	kg/m ³	2750
4.	Geometric model type	---	.stl file
5.	Mould temperature	°C	140
6.	Component weight	gram	343.75
7.	Component size	cm	5 × 5 × 5
8.	Mesh cell size	mm	1 x 1